ICP Imperial College Press
www.icpress.co.uk

Ab initio study of the structural, vibrational and thermal properties of Ge$_2$Sb$_2$Te$_5$

Henry Odhiambo* and Herick Othieno[†]

Department of Physics and Materials Science
Maseno University, P. O. Box 333
Maseno 40105, Kenya
*henod2001@yahoo.com
[†]othieno2@yahoo.com

The structural, vibrational and thermal properties of hexagonal as well as cubic Ge$_2$Sb$_2$Te$_5$ (GST) have been calculated from first principles. The relative stability of the possible stacking sequences of hexagonal GST has been confirmed to depend on the choice for the exchange-correlation (XC) energy functional. It is apparent that without the inclusion of the Te 4d orbitals in the valence states, the lattice parameters can be underestimated by as much as 3.9% compared to experiment and all-electron calculations. From phonon dispersion curves, it has been confirmed that the hexagonal phase is, indeed, stable whereas the cubic phase is metastable. In particular, calculations based on the quasi-harmonic approximation (QHA) reveal an extra heat capacity beyond the Dulong–Petit limit at high temperatures for both hexagonal and cubic GST. Moreover, cubic GST exhibits a residual entropy at 0 K, in agreement with experimental studies which attribute this phenomenon to substitutional disorder on the Sb/Ge/v sublattice.

Keywords: Te 4d electrons; quasi-harmonic approximation; Dulong–Petit limit; phonon dispersion; residual entropy; substitutional disorder; Sb/Ge/v sublattice.

1. Introduction

Alloys along the pseudobinary line $(\mathrm{GeTe})_x(\mathrm{Sb_2Te_3})_y$, the so-called phase-change materials, are known to undergo a reversible and rapid amorphous-to-crystalline phase transformation accompanied by a drastic change in optical as well as electrical properties, opening up opportunities for novel nonvolatile data storage devices [Ovshinsky, 1968; Wuttig and Yamada, 2007; Meijer, 2008; Welnic and Wuttig, 2008]. Ge$_2$Sb$_2$Te$_5$ (GST) is the prototype phase-change material because of its superior performance in terms of speed of transformation (∼50 ns) and its stability in the amorphous phase [Kolobov *et al.*, 2004]. Despite the fact that phase-change

*Corresponding author.

materials are already functional and available in the market, some of their funda-
mental properties are not yet fully understood and are the subject of intense debate
[Welnic and Wuttig, 2008].

GST exhibits two crystalline phases, namely, a metastable cubic phase, which
undergoes the reversible crystalline-to-amorphous phase transition, and a stable
hexagonal phase [Matsunaga *et al.*, 2004; Kooi and De Hosson, 2002]. The hexagonal
phase has P3m1 symmetry and nine atoms per unit cell in nine layers stacked along
the *c*-axis. There are three possible stacking sequences (Fig. 1). Kooi and De Hosson
[2002] have suggested the sequence Te-Ge-Te-Sb-Te-Te-Sb-Te-Ge (hereafter referred
to as phase A), while Petrov *et al.* [1968] have proposed the sequence Te-Sb-Te-Ge-
Te-Te-Ge-Te-Sb (hereafter referred to as phase B), in which the positions of Ge and
Sb atoms are interchanged. Matsunaga *et al.* [2004] have come up with a disordered
phase in which Sb and Ge atoms randomly occupy the same layer resulting in a
mixed configuration.

The cubic phase has a rock-salt-like structure with Te atoms on the anionic sites
and a random distribution of Ge, Sb and vacancies (v) on the cationic sites [Nonaka
et al., 2000; Yamada and Matsunaga, 2000; Kolobov *et al.*, 2004; Park *et al.*, 2005;
Kolobov *et al.*, 2005]. For purposes of implementation, the rock-salt-like structure
has been replaced by an equivalent hexagonal lattice in which the unit cell has 27
atoms and three v arranged along the *c*-axis in the stacking sequence Te-Ge-Te-
Sb-Te-v-Te-Sb-Te-Ge repeated three times (Fig. 2). This arrangement is equivalent
to the atomic stacking along the [111] direction in the corresponding rock-salt-like
structure.

In this work, the influence of the semicore Te 4d electrons on the valence states
has been confirmed in the case of GST. Also, the energy hierarchy of the hexagonal
GST phases has been confirmed to depend on the approximation for the exchange-
correlation (XC) energy functional. The heat capacity and entropy are important
parameters in the thermal modeling of phase-change memory devices, which is
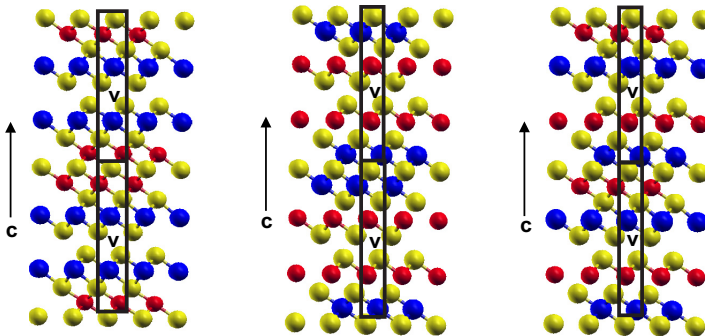

Fig. 1.   (Color online) Arrangement of Te (yellow), Ge (red), Sb (blue) atoms and intrinsic vacan-
cies (v) in phase A (left), phase B (center) and phase C (right) of hexagonal GST. Solid lines
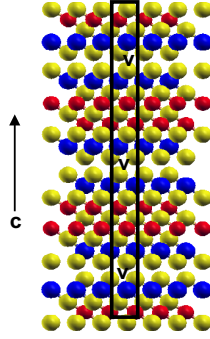indicate the conventional unit cell.

Fig. 2.   (Color online) Arrangement of Te (yellow), Ge (red), Sb (blue) atoms and intrinsic vacancies (v) in rock-salt-like GST. Solid lines indicate the conventional unit cell.

essential for the improvement of device performance in terms of operating speed and power consumption. Tsafack *et al.* [2011] have previously obtained the heat capacity of hexagonal GST from the simulated phonon density-of-states (DoS). In this work, both the specific heat capacity and entropy of hexagonal and cubic GST have been calculated using a novel numerical technique known as the quasi-harmonic approximation (QHA). In particular, lattice vacancies have been shown to have an influence on the thermal properties of hexagonal as well as cubic GST.

2. Computational Details

Electronic structure calculations were performed within the framework of density functional theory (DFT) [Hohenberg and Kohn, 1964; Kohn and Sham, 1965] as implemented in the QUANTUM ESPRESSO package [Giannozzi *et al.*, 2009] which uses plane waves for the expansion of atomic wave functions. The local density approximation (LDA) of Perdew and Zunger (PZ) [Perdew and Zunger, 1981] and the generalized gradient approximation (GGA) of Perdew–Burke–Ernzerhof (PBE) [Perdew *et al.*, 1996] have been considered for the XC energy functional. The electron–ion interactions have been described by nonrelativistic, norm-conserving pseudopotentials. The valence configurations are Ge $4s^2 4p^2$, Sb $5s^2 5p^3$ and Te $5s^2 5p^2$ with the semicore Ge 3d, Sb 4d and Te 4d orbitals being taken into account in the case of the GGA pseudopotential. Studies on the effect of the semicore Te 4d electrons on the valence states is available in recent literature [Lee and Jhi, 2008; Do *et al.*, 2010]. In addition, van Lenthe *et al.* [1996] have pointed out the significant role played by spin–orbit coupling in such heavy atoms as Te, Ge and Sb. However, spin–orbit coupling, which is a relativistic effect, has not been taken into account in this study where nonrelativistic pseudopotentials have been considered.

The Kohn–Sham wave functions were expanded on a plane-wave basis set up to a kinetic energy cutoff of 50 Ry while Brillouin Zone (BZ) integration was performed over an unshifted $8 \times 8 \times 2$ Monkhorst–Pack (MP) [Monkhorst and Pack, 1976] mesh for both cubic and hexagonal GST.

The total energy was calculated for various unit cell volumes using the self-consistent field (SCF) procedure. The resulting energy versus volume data were then fitted to the Murnaghan equation-of-state (EOS) [Murnaghan, 1944] in order to get the equilibrium lattice constants. To obtain the equilibrium atomic positions, the structures were relaxed at the equilibrium lattice constants.

The linear response behavior of the structures was calculated using density functional perturbation theory (DFPT) [Baroni *et al.*, 2001], where the ground-state charge density of the unperturbed system was computed using the SCF procedure with the same kinetic energy cutoff and k-point grid as before. The dynamical matrices (or force constants) were then calculated on a $4 \times 4 \times 4$ grid of q-vectors, with a convergence threshold of the total energy set to 10^{-14} Ry for the hexagonal phase and 10^{-12} Ry for the cubic phase, since the cubic phase takes longer to converge. Finally, the dynamical matrices were transformed from reciprocal space (G) to real space (R).

With the calculated dynamical matrices as input, the heat capacity, entropy and vibrational energy were computed over the temperature range 10–90 K at the equilibrium lattice parameters using the QHA as implemented in the code QHA [Baroni *et al.*, 2010].

3. Results and Discussion

3.1. *Structural properties*

Table 1 shows the total energy after structural relaxation of phases A, B and C of hexagonal GST.

The total energies were calculated using the LDA and GGA for the XC energy functional. It is evident that with the LDA, phase C has the lowest total energy after structural relaxation. However, phase C is marginally lower in energy than phase A, the energy difference between them being about 0.000305 Ry/atom (∼4 meV/atom). On the other hand, GGA calculations suggest that phase A has the lowest total energy after structural relaxation. In this case, the energy difference between phase A and phase C is about 0.000400 Ry/atom (∼5 meV/atom). Other calculations based on DFT with GGA for the XC energy functional also suggest that phase A has the lowest energy [Sun *et al.*, 2006; Sosso *et al.*, 2009]. According to Sosso *et al.* [2009], the difference in energy between phases A and C is about the same order

Table 1.   LDA and GGA total energy (Ry/atom) of phases A, B and C of hexagonal GST after structural relaxation.

	Phase		
	Phase A	Phase B	Phase C
LDA	−13.4262	−13.4259	−13.4267
GGA	−13.2941	−13.2928	−13.2937

of magnitude expected for the free energy contribution (at $300\,\mathrm{K}$) due to the configurational entropy of the disordered phase C $(4/9 \cdot k_B \cdot \log_e (2 \sim 8)\,\mathrm{meV/atom})$. Using the B3PW hybrid functional, Becke [1993] has calculated that phase C is marginally lower in energy than phase A after structural relaxation. Hence, taking into account the configurational entropy, phases A and C seem plausible candidates for hexagonal GST structure. It is clear that the hierarchy in energy between phases A and C seems to depend on the choice for the XC energy functional. In this study, phase A was considered for the hexagonal GST structure.

Table 2 shows the total energy after structural relaxation for hexagonal and cubic GST calculated using LDA and GGA for the XC energy functional. It is evident that hexagonal GST has a marginally lower energy after structural relaxation as expected.

In Table 3, the calculated lattice parameters for hexagonal and cubic GST are shown. Generally, the underestimation of lattice constants (hence overestimation of bulk moduli and overbinding) is a well-known effect of LDA [Sousa *et al.*, 2007]

Table 2. LDA and GGA total energy (Ry/atom) of hexagonal and cubic GST after structural relaxation.

	Structure	
	Hexagonal	Cubic
LDA	-13.42620	-13.42584
GGA	-13.29412	-13.29173

Table 3. Calculated LDA and GGA (in brackets) lattice parameters a (a.u.) and c (a.u.), equilibrium volume V_0 (a.u.^{3}), bulk modulus B_0 (GPa) and its pressure derivative. The last column gives the deviation from experiment.

	This study	Experimental	Others	%dev
Hexagonal GST				
a	7.81 (8.21)	8.034[a]	8.091,[c] 8.072[c]	-2.8% (2.2%)
c	31.38 (32.60)	32.647[a]	32.722,[c] 33.819[c]	-3.9% (-0.1%)
V_0	1720.30 (1900.64)	—	—	—
B_0	56.5 (44.0)	44[g]	—	28.4% (0%)
B_0'	6.21 (3.25)	4[g]	—	55.25% (-18.8%)
Cubic GST				
a	7.80 (7.80)	8.053[b]	8.11,[d] 8.072[f]	-3.1% (-3.1%)
c	95.64 (99.41)	98.544[b]	100.38,[d] 104.121[f]	-2.9% (0.9%)
V_0	5190.92 (5190.96)	—	—	—
B_0	55.3 (59.2)	39[g]	—	41.8% (51.8%)
B_0'	4.74 (3.642)	4[g]	—	18.5% (9%)

[a]Experimental data are from [Kooi and De Hosson, 2002].
[b]Experimental data are from [Park *et al.*, 2005].
[c]Theoretical data are from [Sosso *et al.*, 2009].
[d]Experimental data are from [Park *et al.*, 2009].
[e,f]Theoretical data are from [Da Silva *et al.*, 2008].
[g]Experimental data are from [Krbal *et al.*, 2009].

whereas the overestimation of lattice constants (hence underestimation of bulk moduli and underbinding) is a well-known feature of GGA [Sousa *et al.*, 2007] and this turns out to be true in this study. It is also important to note that the GGA-calculated lattice constants are generally closer to experimental values than the LDA-calculated lattice constants. In LDA calculations, the Ge 3d, Sb 4d and Te 4d orbitals were treated as core states, in contrast to GGA calculations where they were included in the valence states. Without the inclusion of the Te 4d orbitals in the valence states, the lattice constants are found to be underestimated by as much as 3.9% for the hexagonal GST structure. Lee *et al.* [1995] and Khenata *et al.* [2006] have shown that including the Te 4d orbitals in the valence states produced more accurate lattice constants and bulk moduli for Telluride compounds when compared to experiment and all-electron calculations. In another theoretical study, the calculated lattice constants for the rock-salt-like structure of GeTe were found to be smaller than the experimental values by more than 5% without the inclusion of the Te 4d orbitals in the valence states [Do *et al.*, 2010].

3.2. *Vibrational properties*

In Figs. 3 and 4, we present the phonon dispersion curves for hexagonal and cubic GST, respectively, alongside the corresponding vibrational density-of-states (VDOS). It is evident that the two spectra are quite similar in profile, only that the cubic phase has a denser set of curves. This is because the conventional unit cell adopted for the cubic phase has more atoms and hence has more vibrational
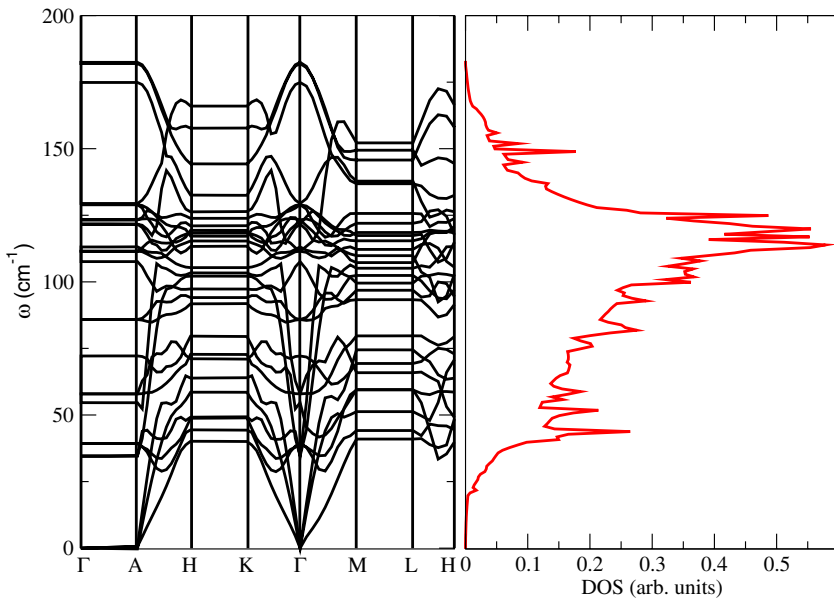

Fig. 3.   Phonon dispersion (left) and the corresponding DoS (right) for hexagonal GST.
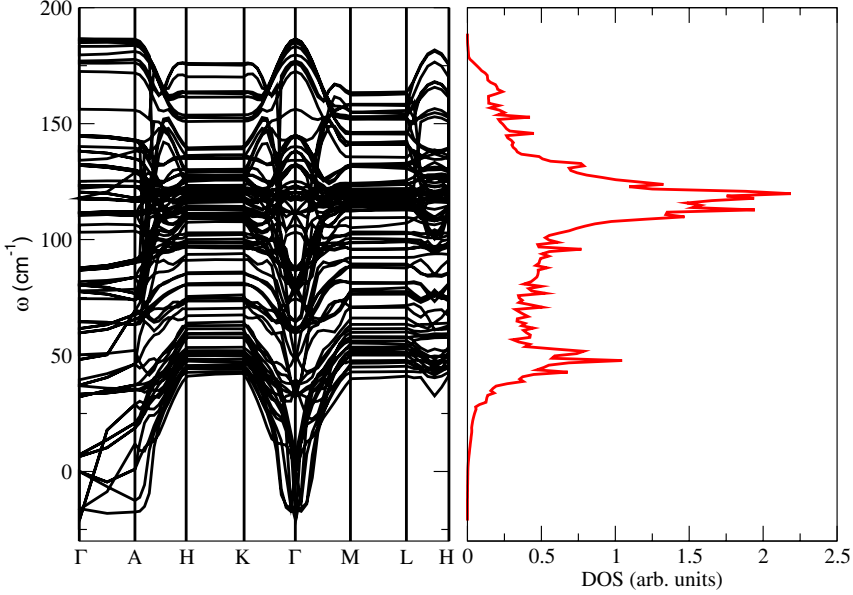
Fig. 4.   Phonon dispersion (left) and the corresponding DoS (right) for rock-salt-like GST.

modes. In particular, the absence of negative frequencies in the phonon spectrum of hexagonal GST is a pointer to the stability of the structure. On the other hand, the presence of negative frequencies in the phonon spectrum of the cubic phase is an indication of the instability of the structure. The cubic phase is often described as metastable and is the phase involved in the reversible crystalline-to-amorphous phase transition that finds application in phase-change memory [Welnic and Wuttig, 2008]. The phonon spectrum for the hexagonal phase shows a set of 27 branches that stretch from $0\,cm^{-1}$ to $182\,cm^{-1}$. This is consistent with nine atoms in the unit cell, each having three modes, giving a total of 27 modes. In addition, the spectrum has six acoustic branches and 21 optical branches. On the other hand, the phonon spectrum for the cubic phase has a set of 81 branches spanning from about $-21\,cm^{-1}$ to about $186\,cm^{-1}$. Again, this is consistent with 27 atoms per unit cell, each atom having three modes, giving a total of 81 modes. The VDOS gives the number of modes per unit frequency per unit volume of real space.

3.3. *Thermal properties*

Figure 5 shows the calculated heat capacity (C_v) as a function of temperature (T) for hexagonal and cubic GST. In both phases, the heat capacity approaches zero as temperature tends towards zero as expected. In addition, the heat capacity should have a cubic dependence on temperature, i.e., $C_v \sim T^3$, at low temperatures as predicted by the Debye model.
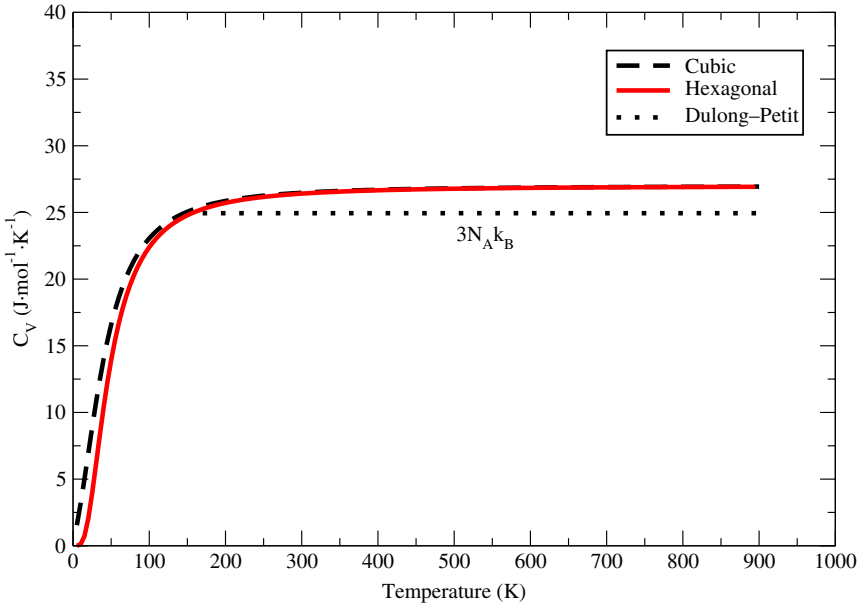
Fig. 5.   Temperature dependence of the specific heat capacity over the range 0–100 K.

However, the heat capacity turns out to be linear at low temperatures for the cubic phase (Fig. 6). Heat capacity can be expressed as the sum: $C_v = (C_v)_{\mathrm{ele}} + (C_v)_{\mathrm{pho}}$, where $(C_v)_{\mathrm{ele}}$ and $(C_v)_{\mathrm{pho}}$ are the electronic and phonon contributions. The electronic contribution has a linear dependence on the temperature, i.e., $(C_v)_{\mathrm{ele}} \sim T$, whereas the photon contribution has a cubic dependence on the temperature, i.e., $(C_v)_{\mathrm{pho}} \sim T^3$. Zalden *et al.* [2014] have estimated that the electronic contribution to the specific heat of the cubic phase is less than $0.08 \, \mathrm{J} \cdot \mathrm{mol}^{-1} \cdot \mathrm{K}^{-1}$, irrespective of the temperature. That is, in the low temperature range, the electronic contribution, $(C_v)_{\mathrm{ele}}$, which is linearly dependent on T, is predominant in the cubic phase. This explains the deviation from the $C_V \sim T^3$ rule. The heat capacity at high temperatures is significantly larger than $0.08 \, \mathrm{J} \cdot \mathrm{mol}^{-1} \cdot \mathrm{K}^{-1}$, an indication that the phonon contribution, $(C_v)_{\mathrm{pho}}$, which varies as T^3, is predominant in that range. It is evident from Fig. 5 that the heat capacity becomes slightly larger than the classical Dulong–Petit limit of $C_V = 3R = 3N_A k_B$ in the high-temperature region. Kalb [2002] and Kuwahara *et al.* [2007] have attributed the slight increase in the heat capacity to point defects such as lattice vacancies.

When point defects are thermally generated, their energy of formation gives an extra contribution to the heat capacity of the crystal. Zalden *et al.* [2014] have shown that the heat capacity of crystalline GST is related to disordered vacancies. It is also evident from Fig. 5 that the cubic phase has a slightly higher heat capacity than the hexagonal phase within the range 0–200 K, in agreement with the experimental work of Zalden *et al.* [2014] who have shown that there is an enhancement of
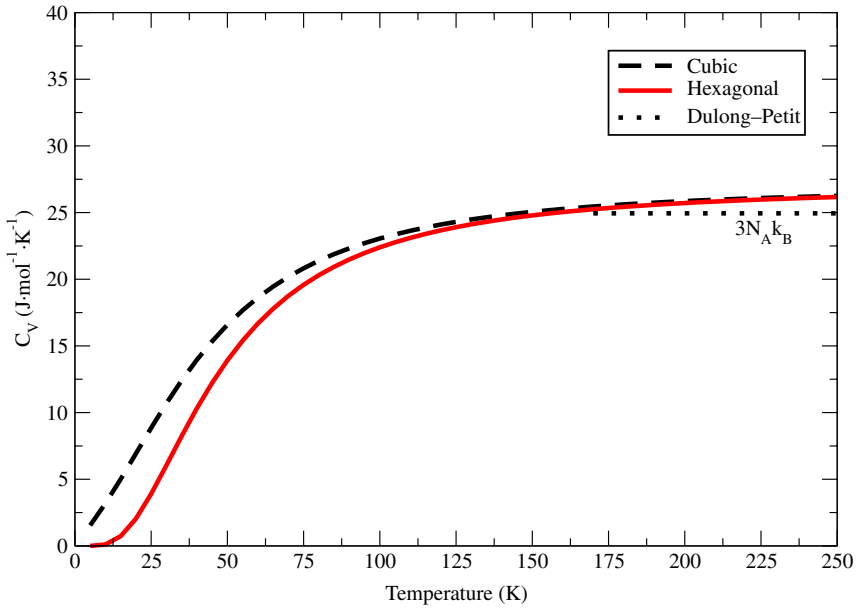
Fig. 6. Behavior of heat capacity curves in the low temperature region.

the heat capacity for the disordered cubic phase as compared to the ordered hexagonal phase. In cubic GST, the lattice vacancies occupy symmetric sites in contrast to hexagonal GST where lattice vacancies are interstitial. Consequently, a higher energy of formation is required to generate vacancies in cubic GST. This accounts for the larger heat capacity in the cubic phase. In Figs. 7 and 8, the theoretical and experimental heat capacities are compared. It is evident that in both hexagonal and cubic GST, the experimental heat capacity is slightly larger than the theoretical heat capacity at high temperatures. According to Tsafack *et al.* [2011], theory does not adequately account for the contribution of lattice vacancies to the heat capacity. Nevertheless, theory and experiment are found to be in agreement within the range 300–500 K for the hexagonal phase and 400–500 K for the cubic phase. Moreover, the theoretical calculations provide an insight into the heat capacity for temperature ranges where experimental data is unavailable, that is, $T < 300$ K for the hexagonal phase and $T < 400$ K for the cubic phase.

Figure 9 shows dependence of entropy on temperature for hexagonal GST. It is clear that the entropy tends towards zero upon cooling to 0 K, in agreement with experimental studies [Zalden, 2012]. In that study, the cubic phase was found to have residual entropy at 0 K. This can be attributed to configurational entropy.

The entropy is defined, in general, by $S = -k_B \cdot \ln(w)$, where w is the number of possible configurations of the system. Thus, single or orderly crystals such as hexagonal GST have no configurational entropy. Compounds from the pseudobinary line $(GeTe)_m(Sb_2Te_3)_n$ are known to possess a large configurational entropy
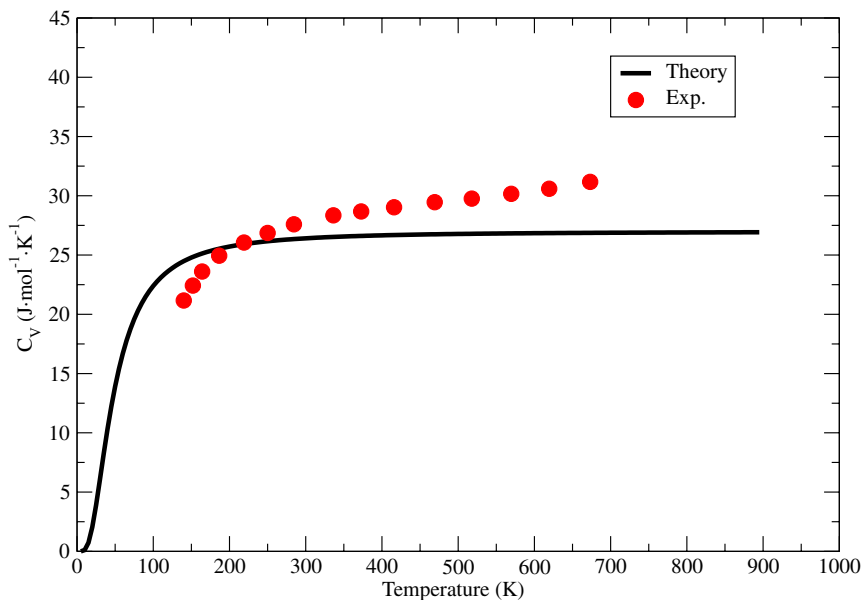
Fig. 7. Comparison of theoretical and experimental heat capacity curves for hexagonal GST. Experimental data is from Kuwahara *et al.* [2007].
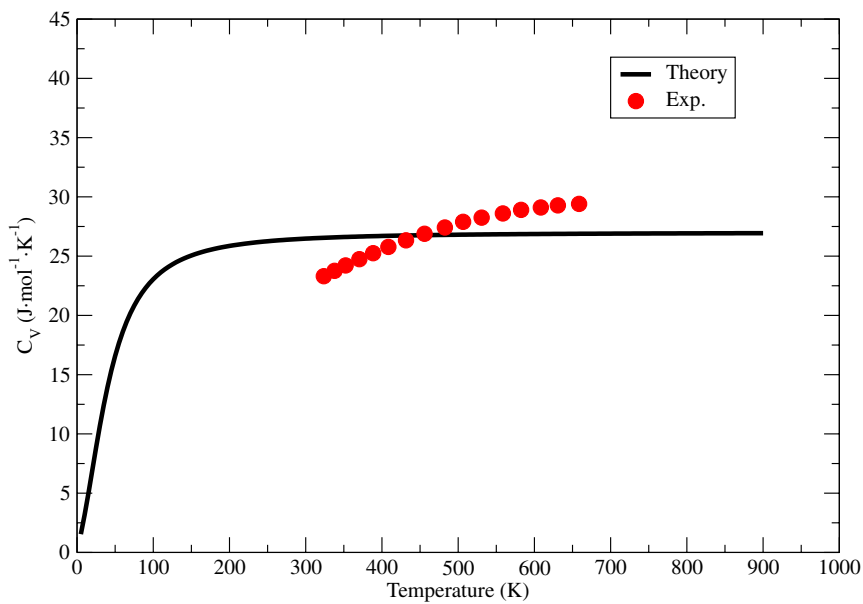

Fig. 8. Comparison of theoretical and experimental heat capacity curves for cubic GST. Experimental data is from to Kalb [2002].
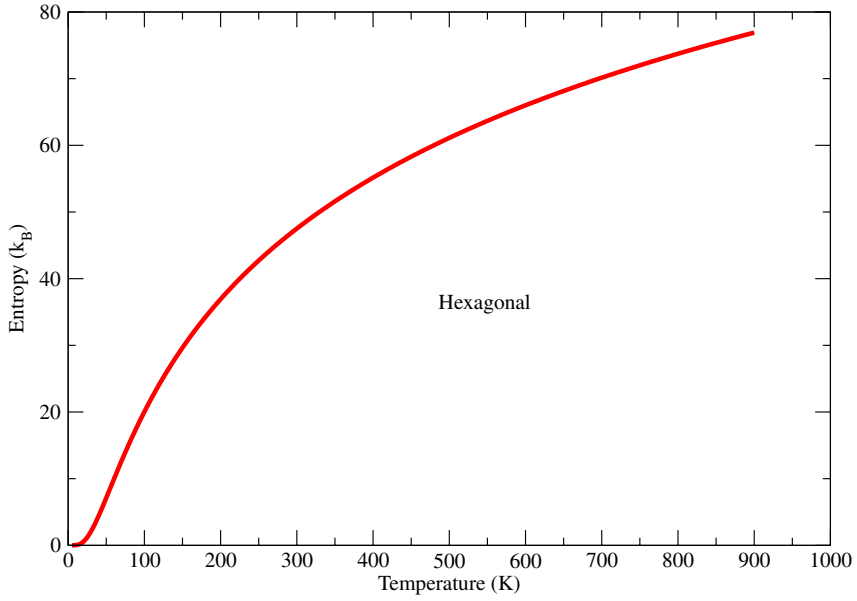
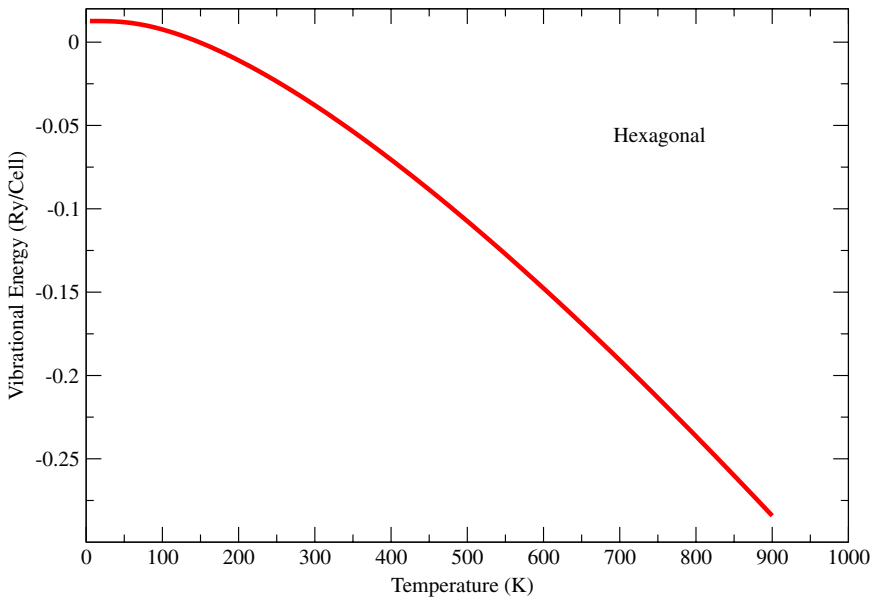Fig. 9.   Entropy as a function of temperature for hexagonal GST.

Fig. 10.   Vibrational energy of hexagonal GST as a function of temperature.

in the metastable cubic phase due to substitutional disorder on the Ge/Sb/v sublattice [Zalden, 2012]. At high temperatures, a system becomes less disorderly and unpredictable. Hence, the entropy increases with temperature.

In Fig. 10, the vibrational energy of hexagonal GST as a function of temperature is shown. All quantum harmonic oscillators undergo fluctuations even in their ground state ($T = 0$ K) and the associated energy is known as the zero-point energy. In this study, a zero-point energy of 0.0126 Ry/atom was calculated for hexagonal GST. Vibrational energy is proportional to temperature. The negative values of vibrational energy indicates that these are bound states, i.e., energy must be expended to cause fluctuations in atomic positions.

4. Conclusion

It is apparent that the hierarchy in energy of the various possible sequences of hexagonal GST depends on the approximation for the XC energy functional, in agreement with previous theoretical studies. Lattice parameters of hexagonal as well as cubic GST have been calculated with and without the inclusion of the semicore Te 4d electrons in the valence states. Lattice parameters are found to be underestimated by as much as 3.9% without the inclusion of Te 4d orbitals in the valence states. The calculated phonon dispersion spectra confirm that indeed hexagonal GST is stable whereas cubic GST is metastable. The specific heat capacity and configurational entropy have been computed using the quasi-harmonic approximation. It is apparent that lattice vacancies have a role in the thermal properties GST. In particular, the energy of formation of lattice vacancies is responsible for an extra heat capacity, pushing the total heat capacity slightly above the Dulong–Petit limit in the high-temperature region. At low temperatures, the electronic contribution to the heat capacity is predominant for the cubic phase. Finally, the cubic phase has a residual entropy at 0 K, which can be attributed to the substitutional disorder in the Ge/Sb/v sublattice.

References

Baroni, S., de Gironcoli, S., dal Corso, A. and Giannozzi, P. [2001] "Phonons and related crystal properties from density functional perturbation theory," *Rev. Mod. Phys.* **73**, 515–562.
Baroni, S., Giannozzi, P. and Esaev, E. [2010] "Thermal properties of materials from *ab initio* quasi-harmonic phonons," *Rev. Min. Geochem.* **71**, 39–57.

Becke, A. D. [1993] "Density functional thermochemistry. III. The role of exact exchange," *J. Chem. Phys.* **98**(7), 5648–5652.

Da Silva, J. L. F., Walsh, A. and Lee, H. [2008] "Insight into the structure of the stable and metastable $(GeTe)_m(Sb_2Te_3)_n$ compounds," *Phys. Rev. B* **78**, 224111.

Do, G. S., Kim, J., Jhi, S. H., Louie, S. G. and Cohen, M. L. "*Ab initio* calculations of pressure-induced structural phase transition of GeTe," *Phys. Rev. B* **82**, 054121.

Giannozzi, P., Baroni, S., Bonini, N., Calandra, M., Car, R., Cavazzoni, C., Ceresoli, D., Chiarotti, G. L., Cococcioni, M., Dabo, I., dal Corso, A., Fabris, S., Fratesi, G., de Gironcoli, S., Gebauer, R., Gerstmann, U., Gougoussis, C., Kokalj, A., Lazzeri, M., Martin-Samos, L., Marzari, N., Mauri, F., Mazzarello, R., Paolini, S., Pasquarello, A., Paulatto, L., Sbraccia, C., Scandolo, S., Sclauzero, G., Seitsonen, A. P., Smogunov, A., Umari, P. and Wentzcovitch, R. M. [2009] "QUANTUM ESPRESSO: A modular and open-source software project for quantum simulation of materials," *J. Phys. Condens. Matter.* **21**, 395502.

Hohenberg, P. and Kohn, W. [1964] "Inhomogeneous electron gas," *Phys. Rev. B* **136**, 864.

Kalb, J. A. [2002] "Stresses, viscous flow and crystallization kinetics in thin films of amorphous chalcogenides used for optical data storage," Ph.D. thesis, I. Physikalichen Institut, Department of Physics, Faculty of Mathematics, Computer Science and Natural Sciences, RWTH Aachen University, Aachen, Germany.

Khenata, R., Bouhemadou, A., Sahnoun, M., Reshack, A. H., Baltache, H. and Rabah, M. [2006] "Elastic, electronic and optical properties of ZnS, ZnS and ZnTe under pressure," *Comput. Mater. Sci.* **38**, 29.

Kohn, W. and Sham, L. J. [1965] "Self-consistent equations including exchange and correlation effects," *Phys. Rev. B* **140**, 1133.

Kolobov, A. V., Fons, P., Frenkel, A. I., Ankudinov, A. L., Tominaga, J. and Uriga, T. [2004] "Understanding the phase-change mechanism of rewritable optical media," *Nature Mater.* **3**, 703.

Kolobov, A. V., Fons, P., Tominaga, J., Frenkel, A. I., Ankudinov, A. L., Yannopoulos, S. N., Andrikopoulos, K. S. and Uruga, T. [2005] "Why phase-change media are first and stable: A new approach to an old problem," *Jpn. J. Appl. Phys.* **44**(1), 3345.

Kooi, B. J. and De Hosson, T. M. J. [2002] "Electron diffraction and high-resolution transmission electron microscopy of the high temperature crystal structures $Ge_xSb_2Te_{(3+x)}$ $(x = 1, 2, 3)$," *J. Appl. Phys.* **92**, 3584.

Krbal, M., Kolobov, A. V., Haines, J., Fons, P., Levelut, C., Le Parc, R., Hanfland, M. [2009] "Initial structure memory of pressure-induced changes in the phase-change alloy $Ge_2Sb_2Te_5$," *Phys. Rev. Lett.* **103**, 115502.

Kuwahara, M., Suzuki, O., Yamakawa, Y., Taketoshi, M., Yagi, T., Fons, P., Fukaya, T., Tominaga, J. and Baba, T. [2007] "Temperature dependence of the thermal properties of optical memory devices," *Jpn. J. Appl. Phys.* **46**, 3909.

Lee, G. D., Lee, M. H. and Ihm, J. [1995] "Role of d-electrons in the zinc-blende semiconductors ZnS, ZnSe and ZnTe," *Phys. Rev. B* **52**, 1459.

Lee, G. and Jhi, S. H. [2008] "*Ab initio* studies of the structural and electronic properties of the crystalline $Ge_2Sb_2Te_5$," *Phys. Rev. B* **77**, 153201.

Matsunaga, T., Yamada, N. and Kubota, Y. [2004] "Structures of stable and metastable $Ge_2Sb_2Te_5$, an intermetallic compound in the GeTe-Sb_2Te_3 pseudobinary system," *Acta Crystallogr. B* **60**, 685–691.

Meijer, G. I. [2008] "Who wins the nonvolatile memory race?," *Science* **319**, 1625.

Monkhorst, H. J. and Pack, J. D. [1976] "Special points for Brillouin zone integration," *Phys. Rev. B* **13**, 5188.

Murnaghan, D. [1944] "The compressibility of media under extreme pressures," *Proc. Natl. Acad. Sci. USA* **30**, 224.

Nonaka, T., Ohbayashi, G., Toriumi, Y., Mori, Y. and Hashimoto, H. [2000] "Crystal structure of GeTe and $Ge_2Sb_2Te_5$ metastable phase," *Thin Solid Films* **370**, 258.

Ovshinsky, S. R. [1968] "Reversible electrical switching phenomena in disordered structures", *Phys. Rev. Lett.* **21**, 1450.

Park, Y. J., Lee, Y. J., Youm, M. S., Kim, Y. T. and Lee, H. S. [2005] "Crystal structure and atomic arrangement of the metastable $Ge_2Sb_2Te_5$," *J. Appl. Phys.* **97**, 093506.

Park, J. W., Eom, S. H., Lee, H., Da Silva, J. L. F., Kang, Y. S., Lee, T. Y. Khang, Y. H. [2009] "Optical properties of pseudobinary GeTe, $Ge_2Sb_2Te_5$, $Ge_1Sb_2Te_5$ and Sb_2Te_5 from ellipsometry and density functional theory," *Phys. Rev. B* **80**, 115209.

Perdew, J. P. and Zunger, A. [1981] "Self-interaction correction to density functional approximations for many-electrons systems," *Phys. Rev. B* **23**, 5048.

Perdew, J. P., Burke, K. and Ernzerhof, M. [1996] "Generalized gradient approximation made simple," *Phys. Rev. Lett.* **77**, 3865–3868.

Petrov, I. I., Imanov, R. M. and Pinsker, Z. G. [1968] "Electron-diffraction determination of the structures of Ge2Sb2Te5 and GeSb4Te7," *Kristallografiya* **13**, 339.

Sosso, G. C., Caravati, S., Gatti, C., Assoni, S. and Bernasconi, M. [2009] "Vibrational properties of $Ge_2Sb_2Te_5$ from first principles," *J. Phys. Condens. Matter.* **20**, 245401.

Sousa, S. H., Hernandes, P. A. and Ramos, M. J. [2007] "General performance of density functionals," *J. Phys. Chem.* **111**, 10439–10452.

Sun, Z., Zhou, J. and Ahuja, R. [2006] "Structure of phase-change materials for data storage," *Phys. Rev. Lett.* **96**, 055507.

Tsafack, T., Piccinini, E., Lee, B.-S., Pop, E. and Rudan M. [2011] "Electronic, optical and thermal properties of the hexagonal and rock-salt-like $Ge_2Sb_2Te_5$ chalcogenides from first principles," *J. Appl. Phys.* **110**, 063716.

van Lenthe, E., Snijders, J. G. and Baerends, E. J. [1996] "Zero-order regular approximation for relativistic effects: The effect of spin–orbit coupling in closed shell molecules," *J. Chem. Phys.* **105**, 6505–6516.

Welnic, W. and Wuttig, M. [2008] "Reversible switching in phase-change materials," *Mater. Today* **11**, 20–27.

Wuttig, M. and Yamada, N. [2007] "Phase-change materials for reversible data storage," *Nature Mater.* **6**, 824–832.

Yamada, N. and Matsunaga, T. [2000] "Structure of laser crystallized $Ge_2Sb_{(2+x)}Te_5$," *J. Appl. Phys.* **88**, 7020–7028.

Zalden, P. E. [2012] "Phase-change materials: Structure, vibrational states and thermodynamics of crystallization," Ph.D. thesis, I. Physikalichen Institut, Department of Physics, Faculty of Mathematics, Computer Science and Natural Sciences, RWTH Aachen University, Aachen, Germany.

Zalden, P., Siegert, K. S., Rols, S., Fischer, S. E., Schlich, F., Hu, T. and Wuttig, M. [2014] "Specific heat of $(GeTe)_x(Sb_2Te_3)_{(1-x)}$ phase-change materials: The impact of disorder and anharmonicity," *Chem. Mater.* **26**, 2307–2312.